

EDF R&D	Validation of <i>Code_Saturne</i> 6.0.2 (Appendix 1)	???-???-2019-???-EN Version 1.0
---------	---	--

Sommaire / Summary

1 Particle-laden Wall Jet (JET_P_2PHI)	1
1.1 Description	1
1.1.1 Geometry and Inlet Conditions	1
1.1.2 Physical Properties of the Fluid	2
1.1.3 Physical Properties of the Particles	2
1.1.4 Reference Publications	2
1.2 Numerical Set-up	2
1.2.1 Mesh	2
1.2.2 Boundary conditions	4
1.2.3 Physical modeling and numerical options	5
1.3 Results obtained	5

EDF R&D	Validation of <i>Code_Saturne</i> 6.0.2 (Appendix 1)	???-???-2019-???-EN Version 1.0
---------	---	--

1 Particle-laden Wall Jet (JET_P_2PHI)

Author: C. Caruyer - modified by Y. Eude (Renuda) le 18/06/2020 **Last update:** 18/06/2020

Key-words: Particle-tracking, Lagrangian Simulation, Turbulent Flow, Two-way Coupling

1.1 Description

The flow is a turbulent air jet along a vertical plane wall, laden with spherical glass particles. This configuration is one of the reference test-cases of the Workshop on two-phase flow predictions organised in Merseburg, Germany in 1996. It was also described in an article [4], and has been of previous numerical studies with former versions of *Code_Saturne* and with the in-house ESTET code [2, 3].

For the 1996-Merseburg workshop, three classes of particles were considered (140 μm glass particles, 50.3 μm nickel particles, and 49.3 μm glass particles) with different mass loads. The present numerical study focuses on the run involving 49.3 μm glass particles, and uses the particle-tracking (Lagrangian) module of *Code_Saturne* [1].

1.1.1 Geometry and Inlet Conditions

Tab. 1.1 summarises the inlet conditions and the geometry of the domain; the geometry is represented in Fig. 1.1.

Section width	150 <i>mm</i>
Section height	350 <i>mm</i>
Jet width <i>b</i>	5 <i>mm</i>
Maximum inlet velocity of the jet	10 <i>m.s</i> ⁻¹
Velocity of the co-current (unladen) flow	2 <i>m.s</i> ⁻¹
Reynolds number for the jet	3300

Table 1.1: Inlet conditions

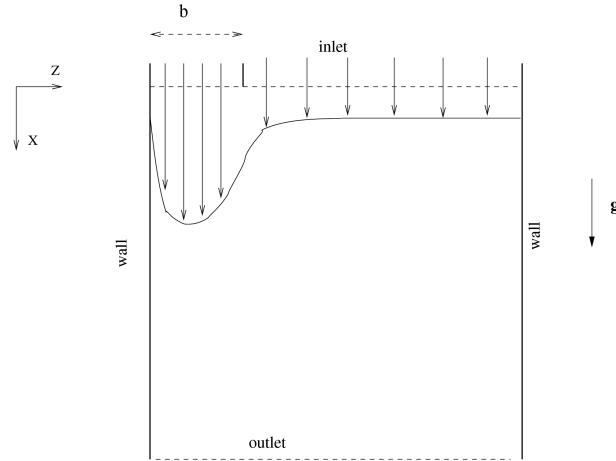


Figure 1.1: View of the geometry of the domain.

1.1.2 Physical Properties of the Fluid

The fluid is air at room temperature.

1.1.3 Physical Properties of the Particles

The particles injected are glass particles; the properties of the particle field are summarised in Tab. 1.2.

Mean diameter d_p	$49.3 \mu m$
Standard deviation of the diameter σ_p	$4.85 \mu m$
Particles density ρ_p	$2590 kg/m^3$
Particle mass load ϕ	0.1

Table 1.2: Particles properties

1.1.4 Reference Publications

- [1] J.P. Minier A. Douce. Modélisation stochastique lagrangienne d'écoulements turbulents diphasiques dans code_saturne. *Rapport EDF HI-81/04/03*, 2004.
- [2] M. Ouraou J.-P. Minier. Module diphasique lagrangien du code estet : calculs de validation et applications industrielles. *EDF internal report, HI-81/01/027/A*, 2001.
- [3] J.P. Minier M. Ouraou. Modélisation lagrangienne des écoulements diphasiques : prise en compte de l'influence des particules sur le fluide dans le module d'estet. *Rapport EDF, HE-44/95/031/A*, 1995.
- [4] K. Hishida Y. Sato and M. Maeda. Effect of dispersed phase on modification of turbulent flow in a wall jet. *J. Fluids Eng., Vol. 11, pp 307-314*, 1996.

1.2 Numerical Set-up

1.2.1 Mesh

The mesh consists in one layer of 4646 hexaedra, and has been generated with the SIMAIL grid-generation software. It is represented in Fig. 1.2 (global view and close-ups of the particle inlet zone). The normalised

EDF R&D	Validation of <i>Code_Saturne</i> 6.0.2 (Appendix 1)	???-???-2019-???-EN Version 1.0
---------	---	--

wall-normal distance of the boundary cell centers along the wall is approximately $y^+ = 11$.

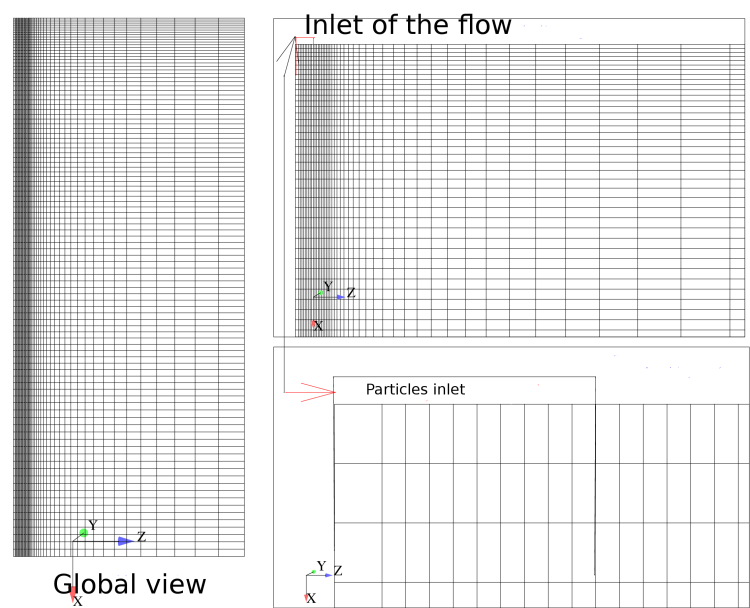


Figure 1.2: View of the mesh

1.2.2 Boundary conditions

Boundary conditions for the air flow

Tab. 1.3 summarizes the characteristics of the air-flow injection given by the available experimental data, with respect to the transverse coordinate. In the numerical simulations, the last column (shear-stress) is not used.

Coordinate z	Mean velocity $\langle u \rangle$ $m.s^{-1}$	Mean velocity $\langle w \rangle$ $m.s^{-1}$	Velocity fluctuation u' $m.s^{-1}$	Velocity w' $m.s^{-1}$	shear-stress $\langle u'w' \rangle$ $m^2.s^{-2}$
mm					
0.8	8.568	0.290	0.733	0.168	0.0084
1	9.069	0.290	0.640	0.171	0.0048
1.2	9.521	0.324	0.455	0.139	-0.0037
1.4	9.828	0.337	0.271	0.125	0.0017
1.6	9.850	0.345	0.211	0.122	0.0045
1.8	9.953	0.353	0.179	0.121	0.0043
2.0	9.944	0.361	0.170	0.119	0.0049
2.2	9.990	0.371	0.166	0.118	0.0043
2.4	9.958	0.365	0.189	0.120	0.0058
2.6	9.906	0.360	0.207	0.118	0.0077
2.8	9.798	0.355	0.254	0.121	0.0096
3.0	9.622	0.349	0.329	0.115	0.0131
3.2	9.494	0.349	0.402	0.136	0.0151
3.4	9.119	0.348	0.512	0.143	0.0199
3.6	8.578	0.328	0.531	0.143	0.0240
3.8	7.896	0.310	0.579	0.142	0.0244
4.0	7.081	0.278	0.592	0.156	0.0224
4.2	5.973	0.237	0.532	0.149	0.0307
4.4	4.821	0.179	0.513	0.159	0.0224
4.6	3.639	0.150	0.418	0.142	0.0167
4.8	2.001	0.069	0.296	0.174	0.0286
5.0	1.136	-0.034	0.180	0.146	0.0191
5.2	0.821	-0.024	0.140	0.116	0.0098
5.4	0.723	-0.053	0.169	0.149	0.0164
5.6	0.736	-0.063	0.162	0.136	0.0127
5.8	0.860	-0.077	0.189	0.143	0.0144
6.0	1.037	-0.086	0.184	0.142	0.0160
6.2	1.113	-0.095	0.179	0.132	0.0139
6.5	1.309	-0.060	0.183	0.117	0.0103
7.0	1.572	-0.052	0.184	0.114	0.0079
7.5	1.711	-0.054	0.169	0.107	0.0078
8.0	1.799	-0.066	0.162	0.114	0.0103
8.5	1.882	-0.045	0.137	0.097	0.0074
9.0	1.920	-0.048	0.145	0.112	0.0110
9.5	1.948	-0.054	0.131	0.111	0.0103
10.0	1.954	-0.056	0.142	0.130	0.0139
11.0	1.995	-0.046	0.136	0.124	0.0126
16.5	2.020	-0.037	0.147	0.140	0.0170
21.0	2.011	-0.041	0.141	0.140	0.0163
31.0	1.995	-0.031	0.151	0.155	0.0203

Table 1.3: Inlet conditions of the air flow

Boundary conditions for the particle field

Tab.1.4 summarizes the characteristics of the particles injection given by the available experimental data. In the numerical simulations, the last column (shear-stress) is not used.

Coordinate z	Volume Fraction	Velocity u_p	Velocity w_p	Velocity fluctuation u_p'	Velocity fluctuation w_p'	shear-stress $< u_p' w_p' >$
mm		$m.s^{-1}$	$m.s^{-1}$	$m.s^{-1}$	$m.s^{-1}$	$m^2.s^2$
0	0.377×10^{-4}	5.544	0	0.352	0.058	0.0017
1	2.236×10^{-4}	8.827	0.179	0.352	0.058	0.0017
1.5	3.014×10^{-4}	9.068	0.206	0.275	0.056	0.0016
2.0	4.306×10^{-4}	9.169	0.221	0.252	0.056	0.0027
2.5	5.689×10^{-4}	8.923	0.220	0.367	0.060	0.0077
3.0	8.567×10^{-4}	8.295	0.223	0.516	0.063	0.0146
3.5	7.099×10^{-4}	7.151	0.206	0.657	0.058	0.0206
4.0	4.520×10^{-4}	6.048	0.190	0.872	0.072	0.0447
4.5	2.184×10^{-4}	4.785	0.195	1.080	0.091	0.0752
5.0	0.377×10^{-4}	5.544	0.504	0.792	0.232	0.1145

Table 1.4: Particle inlet boundary conditions. The values of the particle inlet mean transverse velocity (emphasised values) are set to zero in our simulations.

Nota Bene Like the former numerical studies with *Code_Saturne* and with the ESTET code, considering the uncertainties on the values of the particle mean transverse velocity w_p , it is chosen in the current study to set this inlet variable to zero.

1.2.3 Physical modeling and numerical options

A “two-way” coupling simulation is performed (with particle influence on the flow momentum and turbulent mean variables). The turbulent variables of the flow are resolved with the $k - \varepsilon$ “linear production” turbulence model. The inlet profiles are implemented through interpolations of experimental inlet variables in user-defined functions.

The parameters of the Lagrangian calculation are the following:

- Complete model with turbulent dispersion and crossing trajectory effect (main direction of the flow: the x-axis) starting at the first Lagrangian iteration.
- Numerical scheme: first-order.
- Two-way coupling starting at the first Lagrangian iteration.

The time step is constant, uniform and set to 1×10^{-4} s, sufficiently small to obtain a CFL number lower than 1 for the fluid, and so that the particles do not generally cross more than one cell during a time step. A single calculation is performed. The averaging of the relevant Lagrangian statistics begins from 2000 iterations (where the steady state is reached).

1.3 Results obtained

Fig. 1.3 to Fig. 1.6 represent the numerical results obtained with *Code_Saturne* v6.0.2 compared the experimental data and to the results obtained with *Code_Saturne* v5.0.

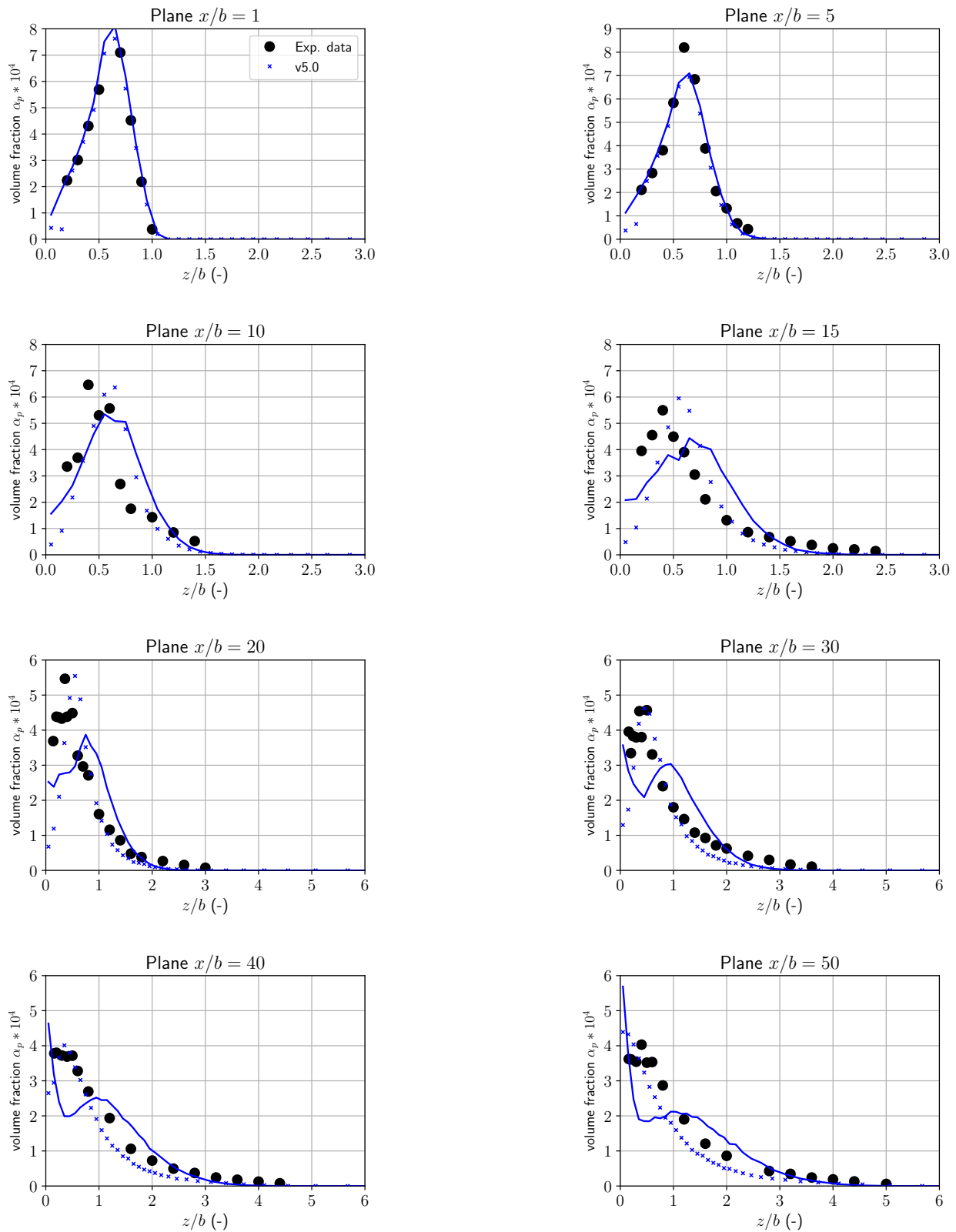


Figure 1.3: Transverse profile of the particle volume fraction at different elevations

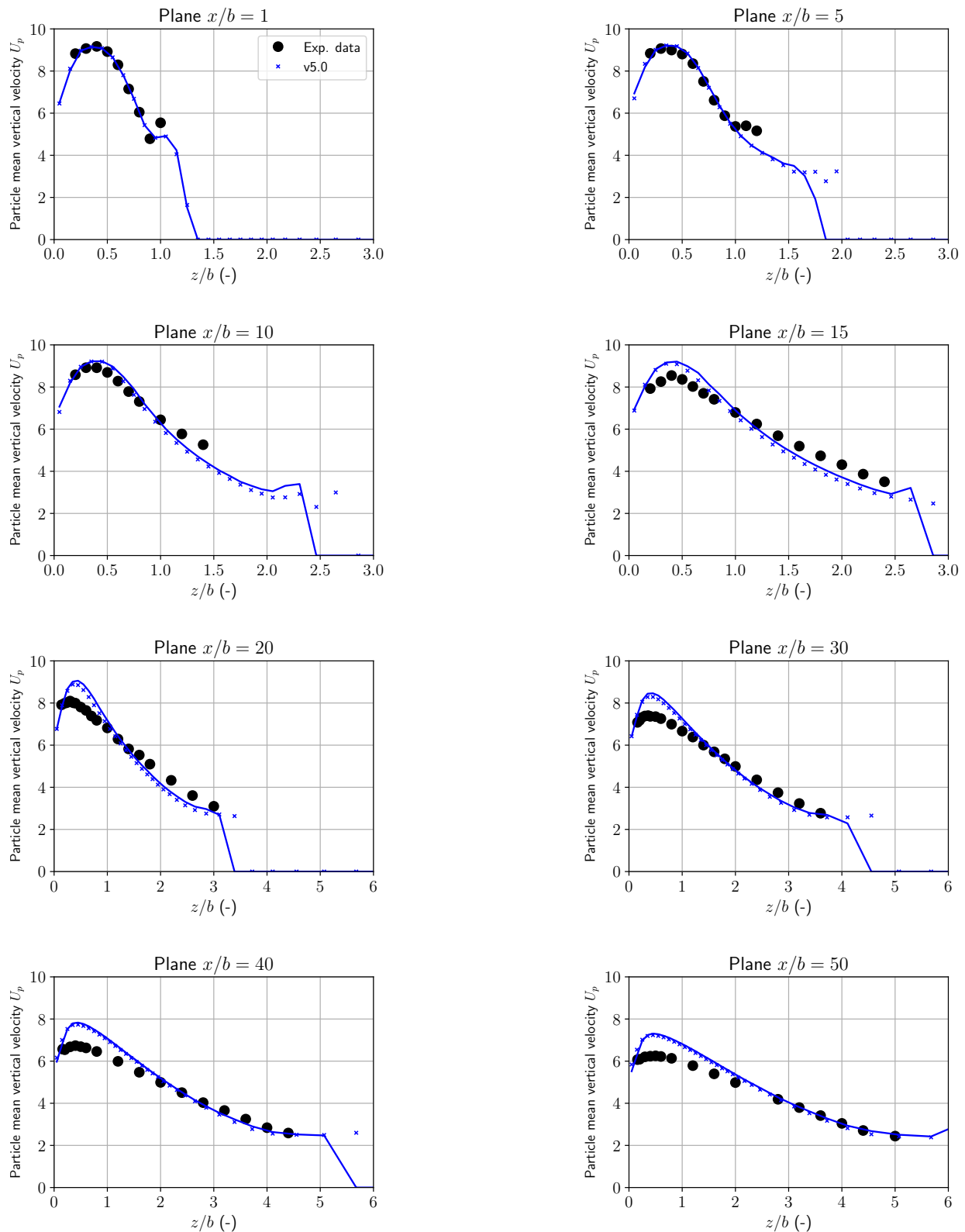


Figure 1.4: Transverse profile of the mean vertical particle velocity at different elevations

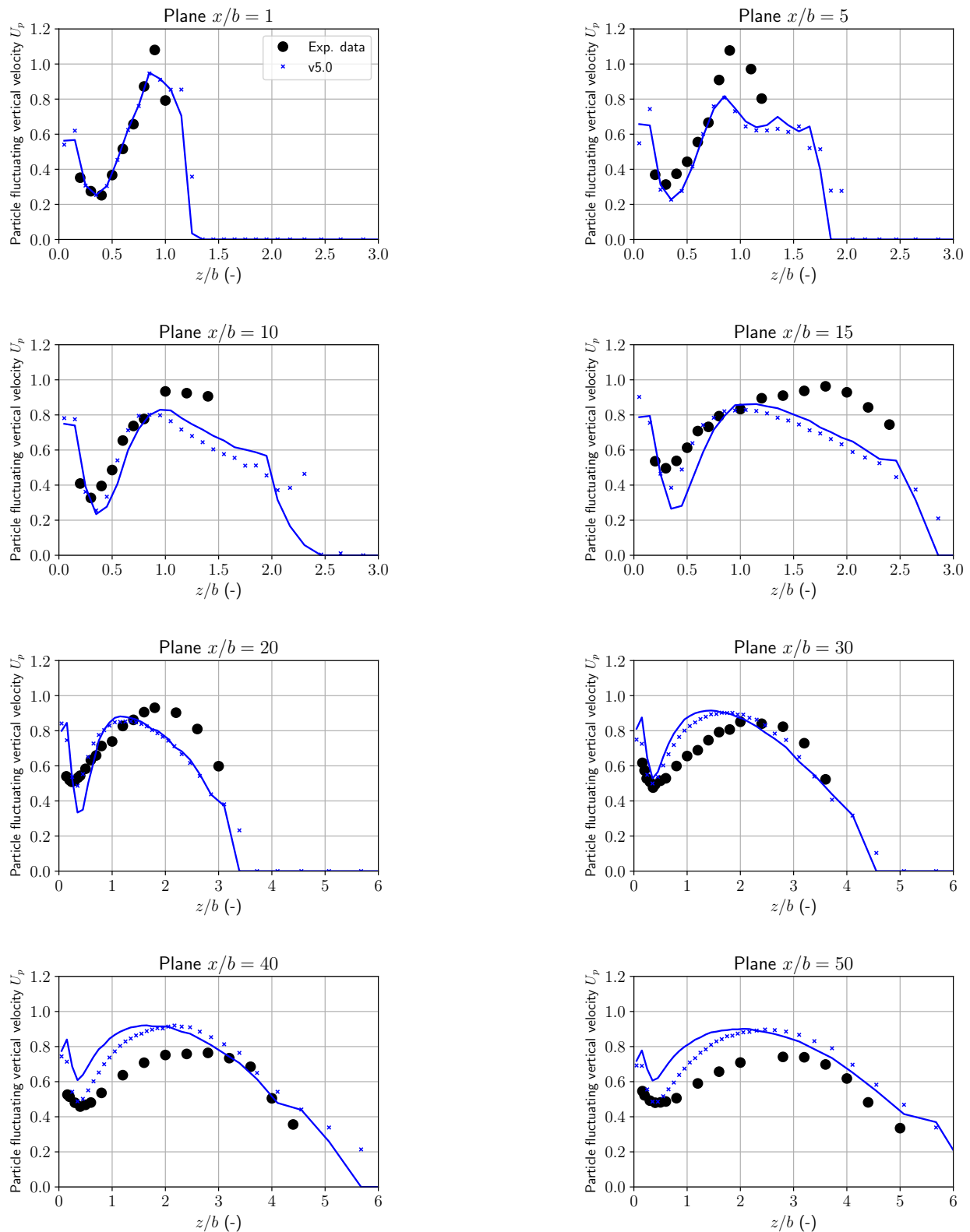


Figure 1.5: Transverse profile of the fluctuating vertical particle velocity at different elevations

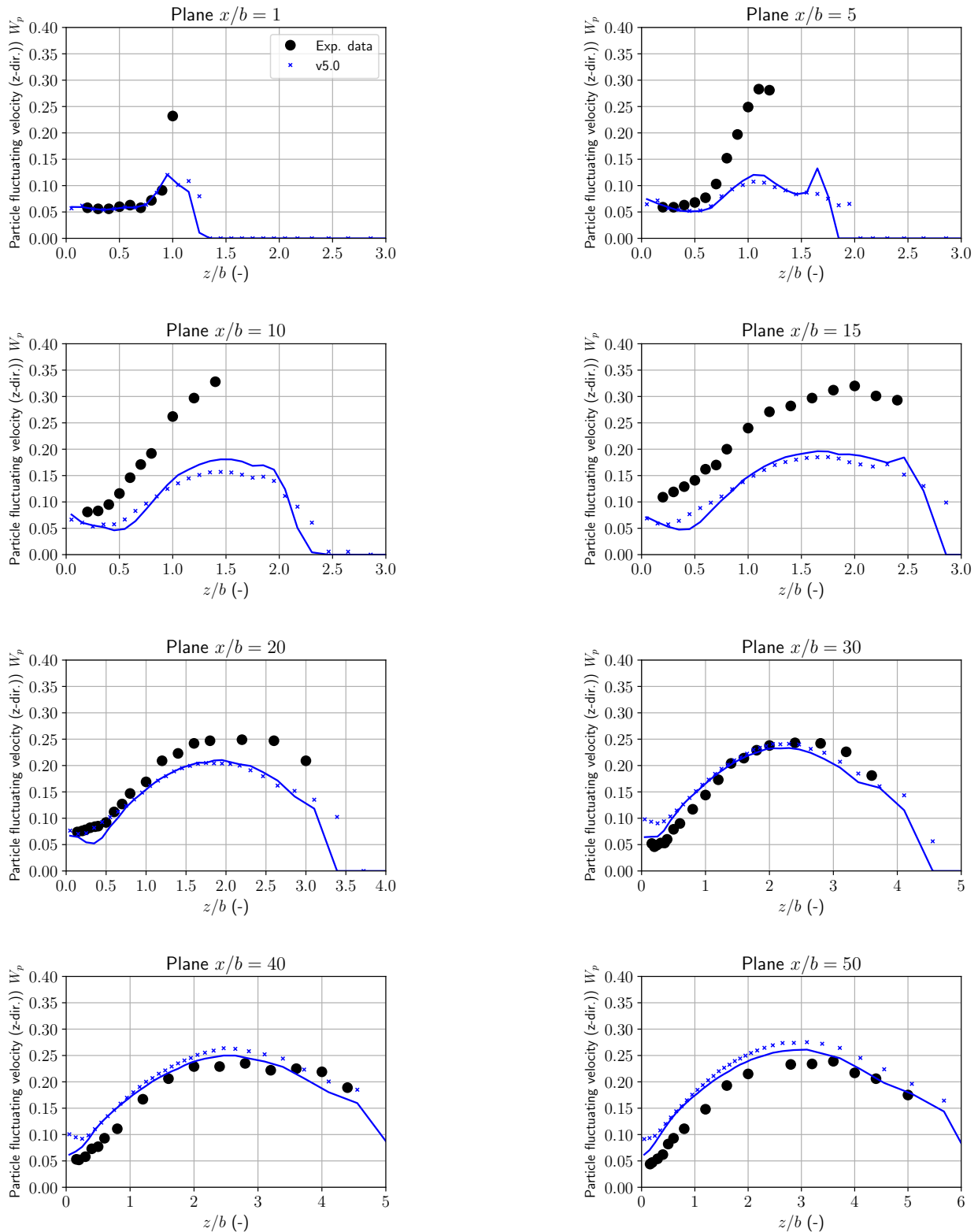


Figure 1.6: Transverse profile of the fluctuating transverse particle velocity at different elevations